Mem. Natl Inst. Polar Res., Spec. Issue, 52, 28–43, 1998

A REVIEW OF RADAR AND SATELLITE BEACON OBSERVATIONS OF ATMOSPHERIC GRAVITY WAVES AT SYOWA STATION

Tadahiko OGAWA

Solar-Terrestrial Environment Laboratory, Nagoya University, Honohara, Toyokawa 442-8507

Abstract: We review the observations of atmospheric gravity waves in the upper mesosphere and the thermosphere that have been carried out at Syowa Station, Antarctica, by means of a meteor radar and satellite beacon wave reception. Occurrence probability and altitude distribution of meteor echoes and mean wind profiles in the upper mesosphere are presented to show that our results are nearly consistent with those in the opposite hemisphere. Gravity waves detected with the meteor radar are well manifested in the sodium abundance (column density) and density perturbations simultaneously measured with a sodium lidar. An evidence is presented that during an auroral substorm, strong winds appeared in accord with a gradual decrease in the sodium abundance. About 400 medium-scale traveling ionospheric disturbances (MSTIDs) in the *F* region were detected with NNSS satellite beacon waves. Statistical analysis indicates that MSTIDs appear quite often during geomagnetically quiet and moderately disturbed conditions and that most of them propagate from south toward the equator. These findings together with the diurnal and seasonal variations of the MSTID occurrences are fairly consistent with previous mid-latitude results. In the future, we need continuous long-term observations at Syowa Station to understand the gravity wave characteristics and the effects of gravity waves upon the global circulation, energy budget in the atmosphere, and thermosphere-middle atmosphere coupling.

1. Introduction

It is believed that long- and short-period gravity waves propagating upward from the lower atmosphere play an important role in the dynamics, energy budget, and general circulation of the middle and upper atmosphere. TSUDA *et al.* (1994) have summarized the gravity wave characteristics in the middle atmosphere by analyzing data from the MU radar at Shigaraki (35°N), medium-frequency (MF) radars at Adelaide (35°S) and Saskatoon (52°N), a lidar at Haute Provence (44°N), and rocketsondes at Uchinoura (31°N). They found that the gravity wave energy in the mesosphere with periods less than about 2 hours is larger in summer than in winter at all the stations and that energy values are generally larger at Shigaraki than at Saskatoon. This study suggests that more observations at other latitudes, in particular at higher latitudes and in the equatorial region, are highly necessary to clarify the global gravity wave characteristics. At high-latitudes, energy input from the magnetosphere during substorm conditions may also disturb the middle atmosphere to induce various complex phenomena that have never been observed at other latitudes (*e.g.*, RÖTTGER and TSUDA, 1995).

Traveling ionospheric disturbances (TIDs) that are wavelike fluctuations of the ionospheric electron density are induced by gravity waves in the neutral atmosphere. There are two classes of TIDs: large-scale TIDs (LSTIDs) characterized by higher speeds (400–1000 m/s) and longer periods (0.5–3 hours) with wavelengths greater than 1000 km, and medium-scale TIDs (MSTIDs) characterized by lower speeds (100–250 m/s) and shorter periods (15 min–1 hour) with wavelengths of several hundred km. MSTIDs appear more frequently than LSTIDs that can be related to specific geophysical events such as auroral substorms. Although auroral sources for generating MSTIDs have attracted the greatest attention (*e.g.*, HUNSUCKER, 1982; BRISTOW *et al.*, 1994), other sources (for example, in the troposphere) are also possible (*e.g.*, HOCKE and SCHLEGEL, 1996).

This paper briefly overviews the radar and satellite observations of atmospheric gravity waves carried out at Syowa Station, Antarctica (69.0°S, 39.6°E). The first observations of winds at the meteor altitudes (80–100 km) were made with a 50 MHz meteor radar for a short period (December 29, 1982–January 15, 1983) (OGAWA *et al.*, 1985). Then winds and gravity waves at the same altitudes were intermittently observed in 1985 with the meteor radar and a 589.0 nm sodium lidar (NOMURA *et al.*, 1987, 1988, 1989; TANAKA *et al.*, 1988; OGAWA *et al.*, 1989). It is stressed that an MF radar is highly necessary to observe the mesospheric winds over Syowa Station on a routine basis.

Beacon waves (150 and 400 MHz) from the polar-orbiting NNSS satellites were received at Syowa Station in 1985 to detect about 400 MSTID events. We briefly summarize the occurrence characteristics of MSTIDs over the Antarctic Continent (OGAWA *et al.*, 1987, 1988).

2. Winds and Gravity Waves at 80–100 km Altitudes

2.1. Capabilities of the Syowa Station meteor radar

Neutral atmospheric winds at meteor altitudes at southern high-latitudes, especially in Antarctica, are not well understood partly because wind measurements there have been extremely scanty (*e.g.*, ELFORD and MURRAY, 1960) in comparison with those at northern high-latitudes. To fill this gap and to study how the Antarctic middle atmosphere differs from or is similar to that at other latitudes, a 50 MHz meteor radar was installed at Syowa Station in 1982 as one of the ground-based study programs in Antarctica for the Middle Atmosphere Program (MAP, 1982–1985) (IGARASHI *et al.*, 1982; OGAWA *et al.*, 1983). The radar, a pulsed-Doppler type with a nominal peak power of 15 kW, was designed as a radar that can detect electron density irregularities appearing often in the disturbed *E* region (OGAWA, 1996). Neutral wind motions in the 80–100 km altitudes were studied using this radar as a meteor radar.

As shown in Fig. 1, the radar has two antenna beams, one toward magnetic south (GMS beam) and the other toward approximately geographic south (GGS beam) with a crossing angle of about 33° (OGAWA *et al.*, 1985). Each beam is formed by using three 14-element coaxial collinear antennas and has a beamwidth of approximately 4° in the horizontal plane and approximately 30° in the vertical plane. In the auroral zone,

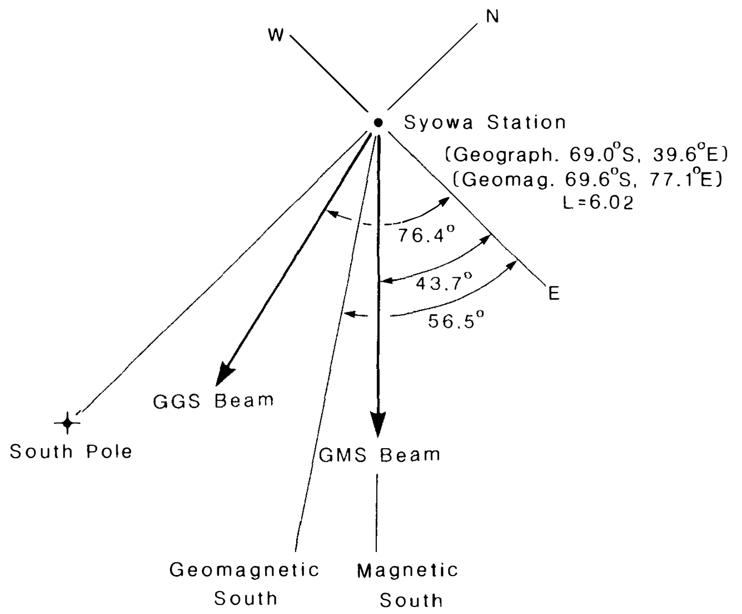

Fig. 1. Two antenna beam directions (GMS and GGS) for 50 MHz meteor radar observations (from OGAWA *et al., 1985).*

meteor echo may be contaminated with radio aurora echo when both echoes appear simultaneously. In order to remove these contaminated echoes, time profile of each echo stored on magnetic tapes was reexamined. As a result, only the underdense echoes decaying exponentially with time were selected for the analysis. Notice that an echo altitude that was determined by using so-called "decay height method" depends on background air temperature and density.

Altitude distribution of the number of echoes (about 2600 echoes in total) obtained from December 29, 1982 to January 15, 1983 is presented in Fig. 2. The echo altitudes range from 70 to 110 km although most of the echoes come from the 80–100 km altitudes with a maximum occurrence around 90 km. The 31.57 MHz Kyoto meteor radar (34.5° N) shows a maximum echo rate at 94 km that is higher by 4 km than our case (ASO *et al.*, 1980). This difference is explained by a fact that a meteor radar with lower frequency can detect echoes at higher altitudes. Figure 3 shows the hourly occurrence of echoes for the GGS and GMS beams together with the total occurrence. Each diagram shows a maximum hourly rate around 0600 LT and a minimum around 2100 LT, a result being nearly consistent with that from the Kyoto meteor radar (ASO *et al.*, 1980).

In Fig. 4, the altitude profile of the mean wind (hourly velocities averaged over the period January 8–15) is compared with other profiles at northern high-latitudes and theoretical results. Note that the standard deviations of the Syowa Station data are quite large (15–25 m/s) mainly due to sparseness of the data points. The Syowa Station zonal wind profile, though the data at 87 km is peculiar, seems to be similar to the CIRA 1972 model and to the Kiruna meteor radar result (GLASS *et al.*, 1978). On the other hand, the meridional winds except at 85 km are between the profiles from Saskatoon (Canada) and Poker Flat (Alaska), confirming that the mean meridional

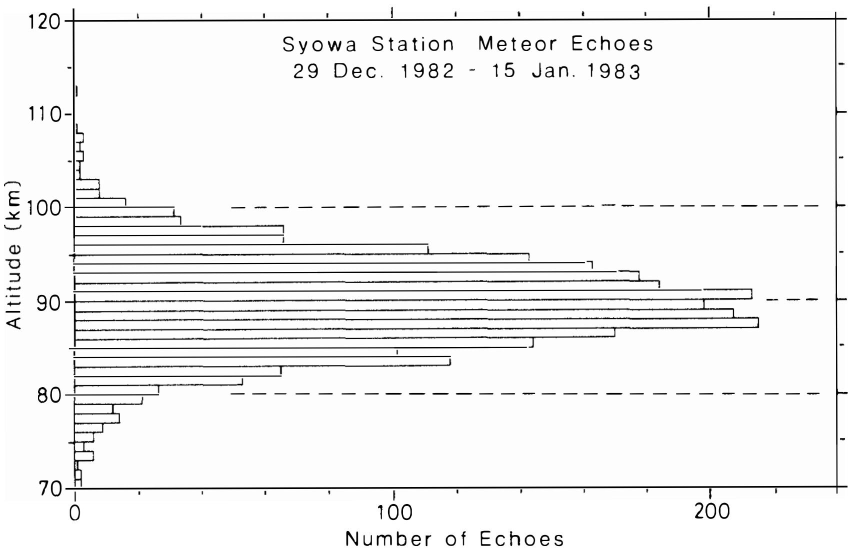

Fig. 2. Altitude distribution of the occurrence number of meteor echoes for the period December 29, 1982–January 15, 1983 (from OGAWA *et al., 1985).*

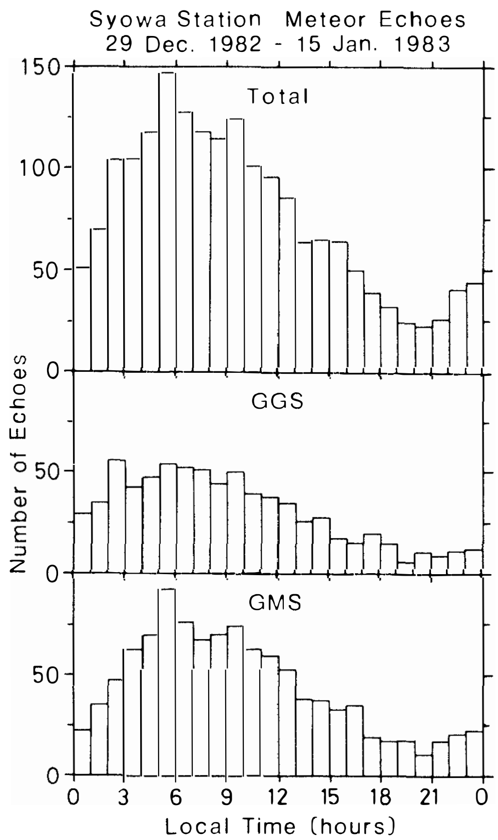

Fig. 3. Hourly distributions of the number of meteor echoes for GGS beam (middle) and GMS beam (bottom) for the period December 29, 1982–January 15, 1983. Total distribution is shown in the top panel (from OGAWA *et al., 1985).*

flow in the summer upper mesosphere is equatorward.

When the ionospheric electric field is large, movement of meteor trail may deviate from neutral wind (REID, 1983). OGAWA *et al.* (1985) presented an evidence of this effect; that is, neutral winds are partly modified by electric fields appearing under

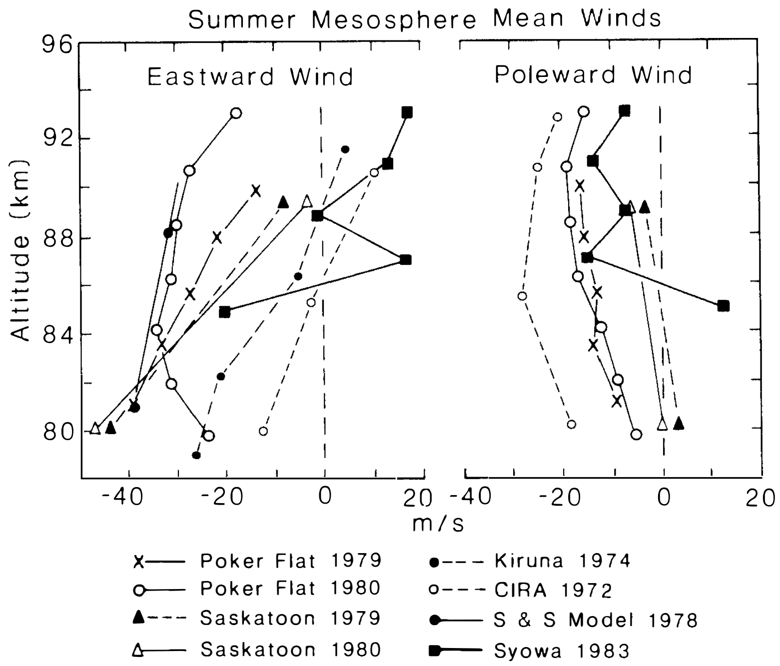

Fig. 4. Comparison of altitude profiles of summer mesospheric mean wind. The profiles except Syowa Station data were adopted from CARTER *and* BALSLEY *(1982) (from* OGAWA *et al., 1985).*

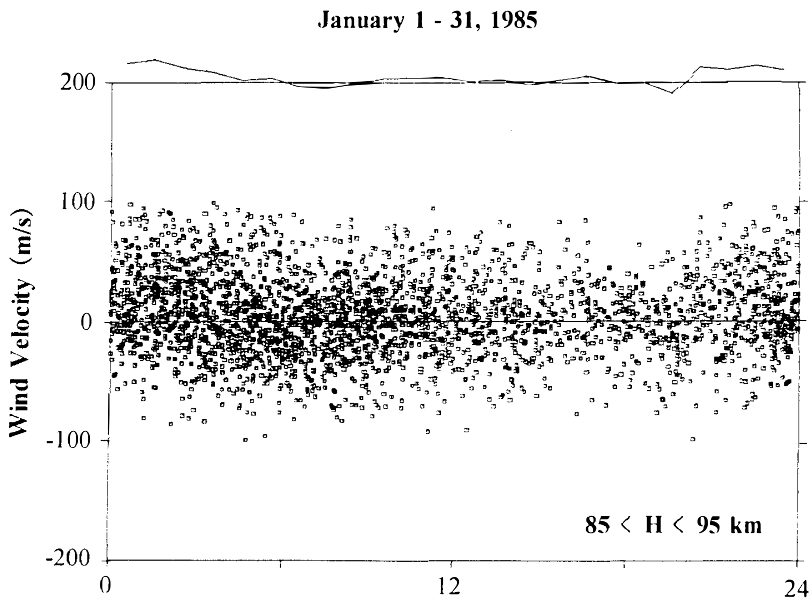

Fig. 5. Scatter plot of wind velocities at altitudes of 85–95 km observed by GMS and GGS beams in January 1985. Hourly-mean wind velocities are shown by the solid line at the upper part (from TANAKA *et al., 1988).*

geomagnetically disturbed conditions.

Figure 5 shows a diurnal scatter plot of wind velocities at the 85–95 km altitudes observed by the GMS and GGS beams in January 1985 (TANAKA *et al.*, 1988). The wind velocities show the diurnal variations although they exhibit a large scatter. The solid curve at the upper part of Fig. 5 shows mean wind velocities calculated for every one hour interval. This velocity shows diurnal and semi-diurnal components with a non-zero diurnal mean value. The amplitudes of these components, however, are smaller than the scatter in the observed velocities. TANAKA *et al.* (1988) suggested a possible role of gravity waves in causing this scatter.

2.2. Upper mesospheric gravity waves

Gravity waves, mostly coming from the lower atmosphere, manifest themselves as modifications of winds and sodium density in the upper mesosphere (80–100 km). Upper mesospheric gravity waves have been observed by a variety of techniques, among which both radar (MF, VHF, and meteor radars) and lidar have been the most powerful tools. Radar can measure neutral wind velocities modulated by gravity waves, while lidar using resonant backscatter from the sodium layer can measure gravity waves as wavelike perturbations of the sodium layer and abundance. Comparison of gravity wave features obtained simultaneously from both techniques is important for understanding the interaction between the upper mesosphere and gravity waves. In this section, we overview some results from the simultaneous measurements of gravity waves with the meteor radar and lidar at Syowa Station, and discuss a relationship between the perturbations of the neutral wind and sodium layer due to gravity waves (OGAWA *et al.*, 1989). It is found that, in addition to long-period (≥ 3 hours) perturbations, short-period (1–2 hours) perturbations of the wind velocity are associated with those of the sodium abundance and its density profile.

In 1985, a lidar system was installed at Syowa Station and observed nighttime sodium layer from the end of March to the middle of October. Detailed descriptions of the system and some results, including temporal and seasonal variations of the sodium layer and gravity wave activities, were given by NOMURA *et al.* (1987, 1988, 1989). From an analysis of the sodium density profiles of 42 nights, NOMURA *et al.* (1989) found that vertical wavelengths, vertical phase velocities and periods range from 4 to 10 km, from 0.5 to 5 km/h and from 1 to 10 hours, respectively. These waves can also be detected with the meteor radar capable of measuring horizontal neutral wind components.

An example is given in Fig. 6 (OGAWA *et al.*, 1989). Time variation of the sodium abundance shown on the bottom in Fig. 6 indicates the fluctuations with periods of 1–2 hours and also of longer than 3 hours (the dashed curve). From an analysis of the sodium density profiles on the same day, NOMURA *et al.* (1987) found the upward-propagating, monochromatic gravity waves with a period of 3 to 4 hours and with a vertical wavelength of about 10 km (*i.e.*, with a vertical phase velocity of about 0.8 m/s).

Time variation of all the N-S wind velocities observed at altitudes (H) of 70–120 km and at slant ranges (R) of 110–600 km appears in the top panel of Fig. 6. In order to see an ordered time variation, only the wind velocities satisfying the conditions of both $70<H<120$ km and $110<R<225$ km and of both $85<H<95$ km and $110<R<225$ km were selected, the results of which are shown in the second and third panels, respectively. The time variation in the third panel exhibits more clearly wavelike

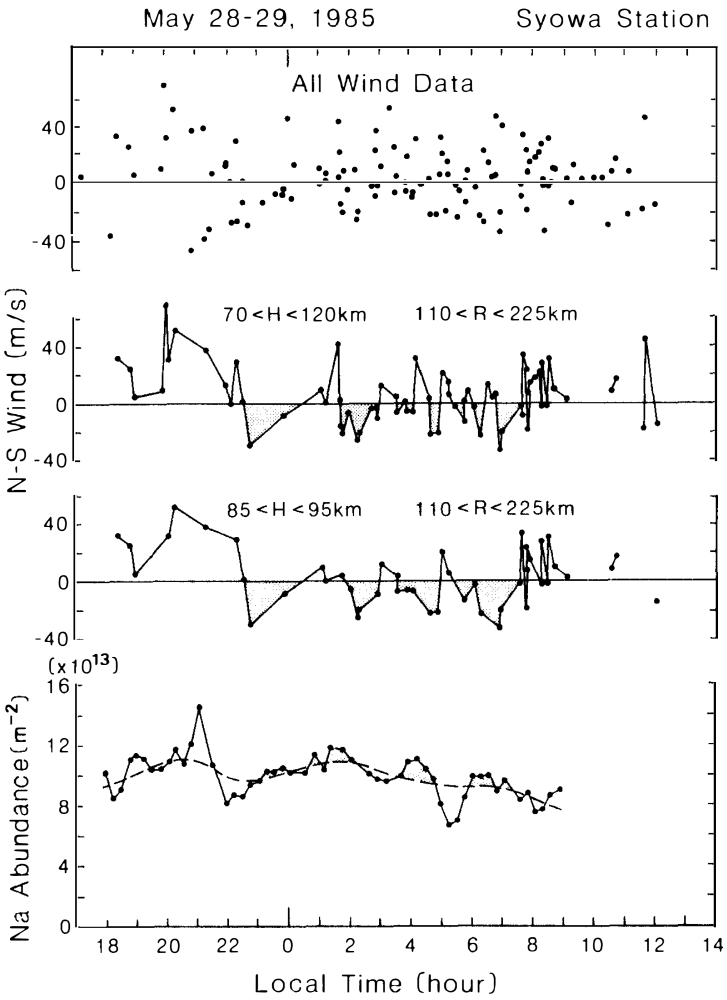

Fig. 6. Time variations of north-south wind velocity (top, second and third) and sodium abundance (bottom) on May 28–29, 1985. Top panel plots all the velocity data at altitudes of 70–120 km and slant ranges of 110–600 km, while second and third panels plot the velocities at limited altitudes (H) and slant ranges (R) as indicated in the figure. Dashed curve superposed upon the abundance represents the smoothed variation (from OGAWA *et al., 1989).*

structure than that in the second panel. This structure can be ascribed to the gravity waves with periods of 1–2 hours and horizontal wavelengths of 120–240 km. Also recognized on this structure, albeit implicitly, are the wave periods longer than 3 hours that give the slowly-varying component of the wind velocity. These longer waves may correspond to the dashed curve of the sodium abundance. It is pointed out that the short-period (<2 hours) structure in the wind velocity is similar to that in the sodium abundance, in particular, for 2200–0800 LT; roughly speaking, when the abundance increases beyond the dashed curve, the wind motion seems to be southward.

We carried out frequency spectrum analyses of the wind velocity, sodium abundance and sodium density to discover the dominant wave periods causing the fluctuations. The results are displayed in Fig. 7. Fairly high correlations among the spectral peaks around 70, 90, 110 and 140 min of the wind velocity, sodium abundance and sodium density spectra are discernible. We conclude that the gravity waves with a variety of periods are well manifested in the wind velocity, sodium abundance and sodium density fluctuations.

NOMURA *et al.* (1987) observed a sodium layer response to an auroral substorm and found that in accord with an auroral breakup, the abundance starts to decrease and the layer does to be compressed from the upper part. A physical process explaining these interesting behaviors is not yet clear. A medium-scale substorm happened on the night of August 16, 1985. Hourly wind velocity and sodium abundance for this event are plotted in Fig. 8. The substorm started around 0120 LT, after which strong northward (equatorward) wind attaining a maximum of 60 m/s appeared. As soon as the *H*-component subsided around 0300 LT, the wind velocity returned to the quiet level. The sudden increase in the wind velocity may be related to ionospheric electric fields

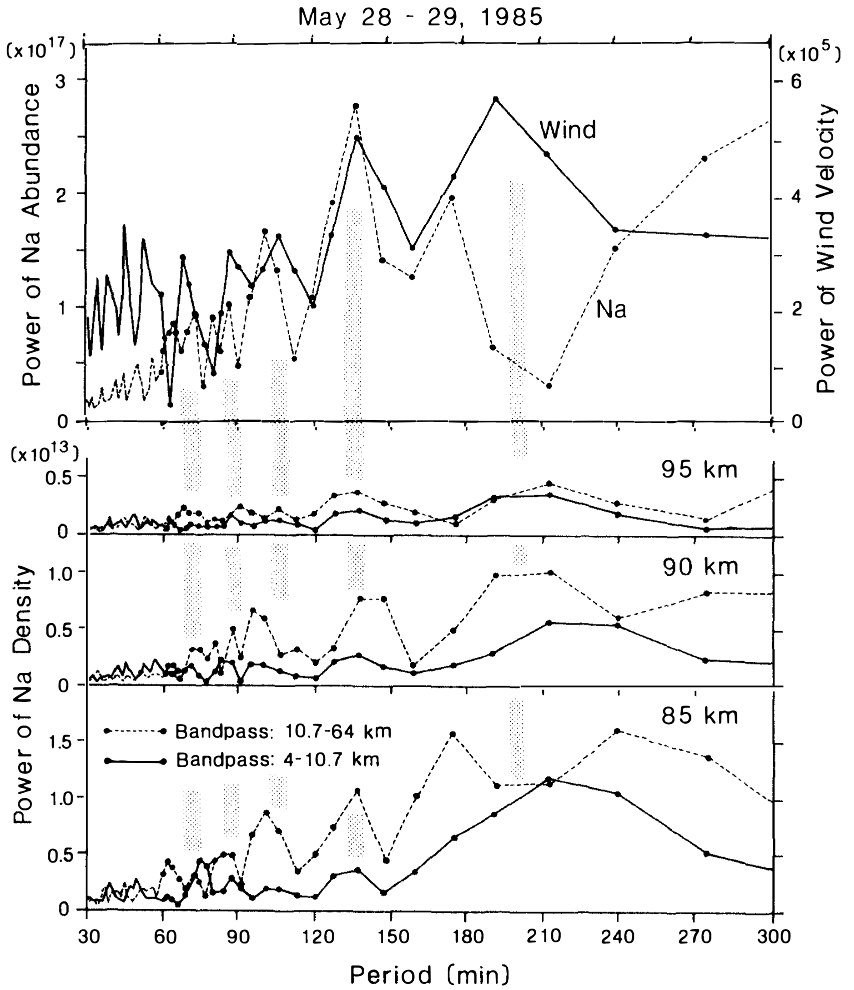

Fig. 7. Frequency spectra of wind velocity and sodium abundance (top) and sodium densities at 95 (second), 90 (third) and 85 (bottom) km bandpass-filtered between 10.7 and 64.0 km (dashed curves) and between 4.0 and 10.7 km (solid curves) in vertical wavelength on March 28–29, 1985 (from OGAWA et al., 1989).

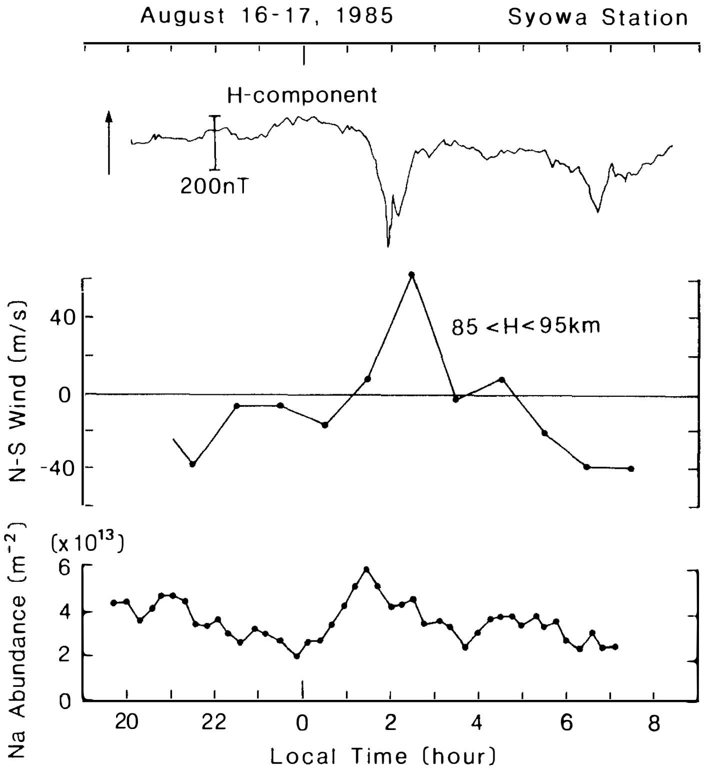

Fig. 8. Time variations of geomagnetic H-component at Syowa Station (top), hourly-averaged north-south wind velocity (middle) and sodium abundance (bottom) on August 16–17, 1985 (from Ogawa et al., 1989).

which can modify neutral winds when strong electric fields penetrate toward lower altitudes (85–95 km) (Reid, 1983). Ogawa *et al.* (1985) presented examples showing that wind velocities sometimes exceeded 100 m/s during disturbed conditions. Prikryl *et al.* (1986) demonstrated that meteor drifts near midnight for disturbed days were predominantly equatorward with velocities up to 100 m/s and were well correlated with simultaneous $E \times B$ drifts in the E region. In Fig. 8, the wind velocities at the maximum substorm phase have an equatorward component, and the sodium abundance starts to decrease in accord with the substorm onset, which agrees qualitatively with the observation of Nomura *et al.* (1987).

2.3. Planned MF radar experiment

Our current understanding of the dynamics of the middle atmosphere over Syowa Station is still very poor, mainly because of lack of equipment suitable for continuous wind observations. To overcome this, we have proposed an MF radar experiment for exploring the atmosphere between 60 and 100 km (Ogawa, 1995). The objectives of this experiment are to study: (1) dynamics of the Antarctic middle atmosphere (mean winds, tidal oscillations, planetary waves, and gravity waves), (2) mesosphere-thermosphere coupling, (3) comparison of the Antarctic middle atmosphere with the Arctic middle atmosphere, and (4) air circulation, tidal modes, planetary wave modes, and climatology of gravity waves on a global scale by participating in the worldwide atmospheric radar network. The National Institute of Polar Research will start the MF radar experiment in 1999. Recently, a possibility of detecting meteor echoes with the SuperDARN HF radars has been discussed by HALL *et al.* (1996; private commun.). The MF radar combined with the two SuperDARN HF radars at Syowa Station will greatly contribute to the better understanding of the Antarctic middle atmosphere.

3. Medium-Scale TIDs in the Thermosphere

Traveling ionospheric disturbances (TIDs), *i.e.*, wavelike fluctuations of the ionospheric electron density induced by gravity waves, have been observed by various methods including vertical-soundings, incoherent scatter radars, HF Doppler measurements, total electron content measurements, and in situ measurements of electron density. In this section, we describe some results from the medium-scale TID (MSTID) observations carried out at Syowa Station from March 1985 to January 1986 (OGAWA *et al.*, 1987, 1988). MSTIDs were detected on differential-Doppler records when we received the 150 and 400 MHz radio beacons from six NNSS satellites. The differential-Doppler shift (Δf) is proportional to the rate of change of the phase path length through the ionosphere. Since Δf includes information on total electron content, oscillatory features of the ionosphere due to TIDs are manifested as oscillations on Δf records.

Figure 9 shows an example of the chart recording of Δf obtained on August 26, 1985. There were seven successive satellite passes (1–7) during 1230–1510 UT when the geomagnetic H-component was very quiet (K-index at Syowa Station $=1$) and showed no substorm activity, at least, over Syowa Station ($Kp=2+$). Except pass number 4, oscillation of Δf is clearly seen on each pass. It is believed that such oscillations are due to TIDs. Predominant oscillation periods of 1–2 min observed in Fig. 9 can be converted into spatial wavelengths of 300–600 km in the F region, by taking into account the high orbiting velocity of satellite (about 7.4 km/s) and far lower velocity of TIDs less than 1 km/s. Therefore these oscillations can be categorized as MSTIDs although we do not know their phase velocities and wave frequencies by the present observation technique.

Δf records of more than 10000 passes were obtained for a 10-month observation period, covering all local times, seasons and various geomagnetic activity conditions. Of these, MSTIDs such as those shown in Fig. 9 were recognized on 428 passes. Here Δf oscillation was judged as an MSTID when its oscillation lasted for two cycles or more on the chart records.

As illustrated in Fig. 10, an MSTID has a negative wave front tilt in the propagation direction of about $-40° \pm 10°$ (DAVIES and JONES, 1971). Relying on this feature, we can expect that TID is best detected when the elevation angle of radio path from NNSS to the observer coincide with the wave front tilt. Actually, the oscillations on passes 2 and 7 in Fig. 9 were detected around the beginning of each south-bound pass, namely, to the north of Syowa Station. These oscillations can be understood as caused by the northward- (equatorward-) propagating gravity waves. In order to determine whether MSTIDs were detected to the north or south of Syowa Station, 320 MSTID events were extracted, which showed the maximum satellite elevation angles

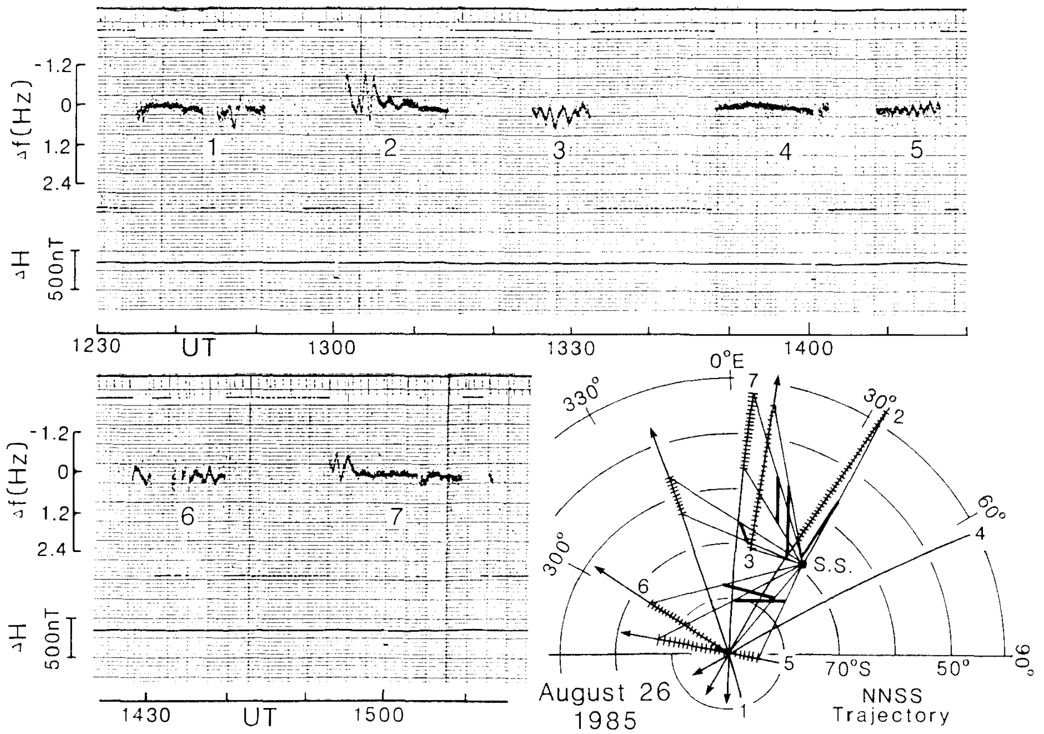

Fig. 9. Chart recording of differential-Doppler (Δf) and geomagnetic H-component (ΔH) at Syowa Station on August 26, 1985 ($K=1$; $Kp=2+$). Subsatellite tracks (curves with arrow) of seven NNSS satellite passes are also shown on the geographic coordinates. Occurrence interval of Δf oscillation is indicated by short bars on the track. Since TIDs are phenomena mainly in the F region, 300 km subionospheric track (defined as the intersection points of the radio path with a shell at 300 km altitude) during the interval of oscillation occurrence on each pass is indicated by heavy solid line (from OGAWA et al., 1989).

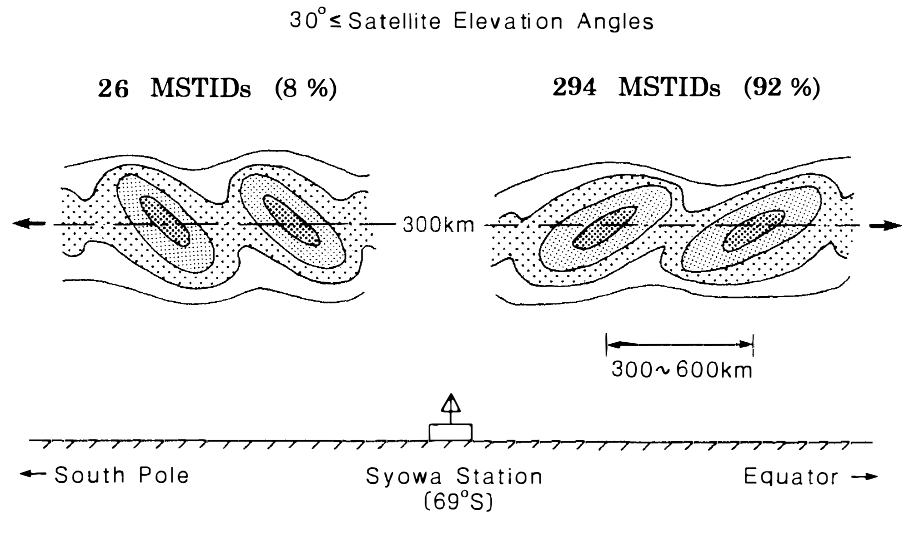

Fig. 10. Schematic illustration of medium-scale TIDs propagating equatorward (northward) and poleward (southward).

larger than 30°. As a result, MSTIDs were detected to the north (equator) for 92% of the events and to the south (pole) for 8%, thus suggesting that most of MSTIDs were propagating from south to the equator (Fig. 10). This conclusion is consistent with the mid-latitude result by EVANS *et al.* (1983) who pointed out that in winter and the equinoxes the majority of TIDs were seen to the equator of Millstone Hill (42.6°N). Extremely predominant equatorward propagation of our TIDs, however, may not necessarily reflect the actual situation of internal gravity waves. HOOKE (1970) found from the calculation of the F_2 region response to internal gravity waves that the response has high anisotropy depending on wave parameters, magnetic dip and ionization density gradient. From his calculation, it is expected that MSTIDs to the north of Syowa Station (dip = 64.8°) are more easily detected than those to the south of Syowa Station, a result being consistent with our result.

Occurrence numbers of TIDs (B) and K-indices (A) are plotted in Fig. 11 as a function of K-index at Syowa Station. B/A shown in the upper panel of Fig. 11 represents the TID occurrence probability at a given K-index. It is clear from this figure that the occurrence probability decreases monotonically with increasing K-index. However, one important observational fact must be borne in mind in understanding this result: with increasing geomagnetic activity, Δf, in particular in the nighttime, tends to be more scattered because the 150 and 400 MHz radio waves are subject to stronger ionospheric scintillations, resulting in frequent difficulty of identifying oscillatory structures on the chart records. This fact means that the occurrence probability in Fig. 11 may underestimate the real probability when K-index is large, say $K \geq 3$. Nevertheless, one conclusion is that the MSTIDs appear with high probability even under geomagnetically quiet conditions ($K = 0, 1$, and 2), thus suggesting a role of atmospheric gravity waves not produced by auroral activities. One point to be noted is that when K-index was low, TID due to auroral activity in other regions might reach Syowa Station. In order to check this possibility, a Kp-index dependence of the occurrence probability was also examined: it was found that the Kp dependence is almost similar to the K dependence.

Figure 12 shows the occurrence number of TIDs versus month. The TID activity is highest in August (in southern winter) and lowest in January. This finding is partly consistent with the result from Millstone Hill (EVANS *et al.*, 1983). HIROTA (1984) found from meteorological rocket data that the gravity wave activity in the middle atmosphere shows a notable annual cycle at higher latitudes with a maximum in wintertime while it shows a semiannual cycle at lower latitudes with maximums around equinoxes. This finding may explain a part of our result in Fig. 12: that is, our seasonal TID activity can be explained by the seasonal gravity wave activity in the high-latitude middle atmosphere. It is noted, however, that gravity waves originated in the lower atmosphere must suffer from dissipation and/or filtering during their upward propagation, and as a result, a part of them can reach the F region height. Other factors to be noticed are: (1) certain biases inherent to the total electron content technique for atmospheric wave observation (GEORGES and HOOKE, 1970), (2) high anisotropic ionospheric response to gravity waves (HOOKE, 1970), and (3) dependence of a detectability of gravity waves on ambient electron density (EVANS *et al.*, 1983). Because of these factors, our statistical result may not necessarily reflect the actual nature

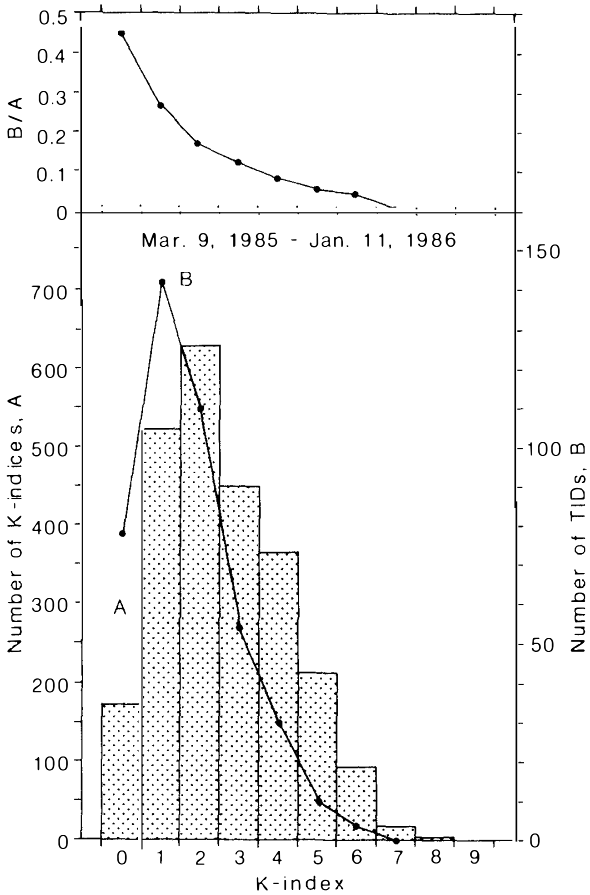

Fig. 11. Occurrence number of medium-scale TIDs (B) and histogram of K-indices (A) versus Syowa Station K-index (lower) and B/A showing the occurrence probability for a given K-index (upper) (from OGAWA *et al., 1987).*

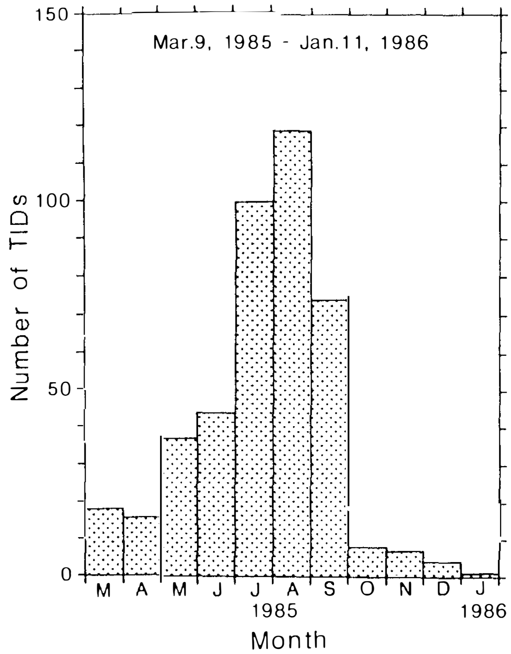

Fig. 12. Seasonal variation of the occurrence number of medium-scale TIDs (from OGAWA *et al., 1987).*

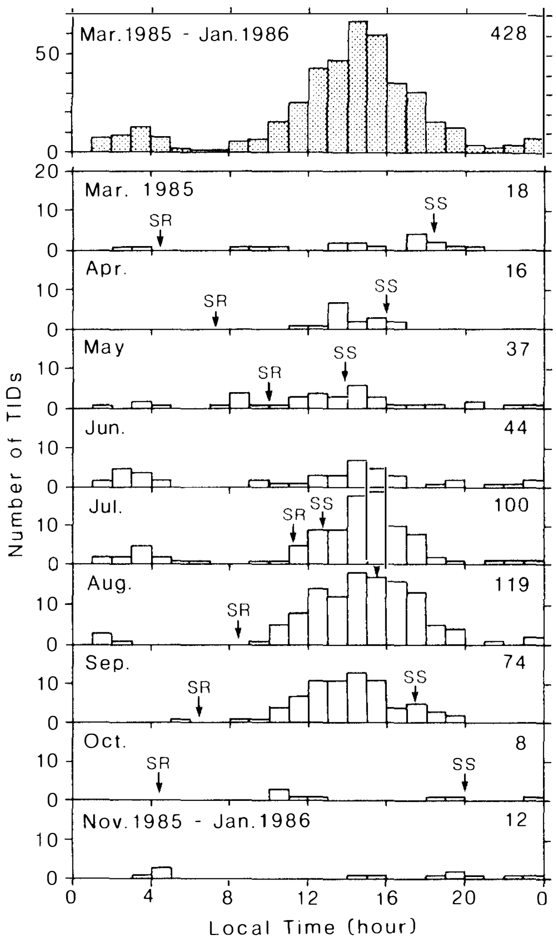

Fig. 13. Diurnal variations of the occurrence number of medium-scale TIDs in each month (bottom) and for ten months (top). The occurrence number of TIDs in each month is also indicated. SR and SS denote the mean local sunrise and sunset hours, respectively. Note no sunshine in June (from OGAWA *et al., 1987).*

of atmospheric gavity waves at ionospheric heights.

Figure 13 shows the diurnal distributions of the occurrence number of MSTIDs in each month (bottom panel) and for the full experimental period (top panel). In the top panel, there are two maximum occurrences: one around midnight and the other in the afternoon hours. The midnight increase may be partly due to auroral activities over Syowa Station because of its location under the auroral oval during disturbed conditions. In fact, most of the TIDs around midnight were observed when K-index exceeded 3. On the other hand, the afternoon increase cannot be ascribed only to auroral activities since many TIDs were observed when K- or Kp-index was very low. The daytime increase was found by EVANS *et al.* (1983) who attributed this increase to the detectability (that is, enhanced ambient electron density) of TIDs.

MSTIDs in high- and mid-latitudes have been often investigated in relation to auroral activities like perturbations in the auroral electrojet (Lorentz force and/or Joule heating), auroral particle precipitation, and supersonic movement of auroral arcs (*e.g.*, HUNSUCKER, 1982). The results presented here, however, show that a large number of MSTIDs were observed even under no and low auroral activities.

4. Concluding Remarks

First, we have presented the occurrence probability and altitude distribution of meteor echoes and the mean wind profiles during December 29, 1982–January 15, 1983. Our results are nearly consistent with those in the opposite hemisphere. Then, the simultaneous measurements of high-latitude upper mesospheric gravity waves using the 50 MHz meteor radar and sodium lidar have been presented to find that the short-period (1–2 hours) and long-period ($\geq$2 hours) perturbations of the wind velocity due to gravity waves are well manifested in the sodium abundance and sodium density perturbations. This fact suggests that the response of the neutral wind to gravity waves is fundamentally consistent with the sodium layer response. It has been also demonstrated that strong winds of 60 m/s appeared in accord with the gradual decrease in the sodium abundance during an auroral substorm. A mechanism explaining this causal relation is unknown and should be explored in the future. Finally, we have introduced 428 MSTID events that were detected at Syowa Station from March 1985 to January 1986. The statistical analysis tells that (1) MSTIDs quite often appear during geomagnetically quiet and moderately disturbed conditions, and their occurrence does not seem to increase with increasing geomagnetic activity, (2) they attain a maximum activity in winter and a minimum in summer, (3) diurnal variation shows a maximum occurrence around 1400–1600 LT with a second maximum around midnight, and (4) most of MSTIDs propagate from south toward the equator. These findings are fairly consistent with the previous mid-latitude results.

We have reviewed the wind and gravity wave observations in the 80–100 km altitudes. However, because of the insufficient data-bases constructed from a limited number of observations, it has been impossible to examine in detail mean winds, long-scale waves such as atmospheric tides and planetary waves, and climatology of gravity waves. In the future, such studies will be highly necessary for understanding the global circulation, energy budget in the atmosphere, and thermosphere-middle atmosphere coupling, although they require a large amount of data obtained through continuous long-term observations. The polar middle atmosphere may be greatly disturbed during substorm conditions. To know how this atmosphere behaves under such conditions, in addition to the MF radar, we need other radio and optical remote sensors at Syowa Station capable of measuring the physical parameters in the thermosphere and the mesosphere.

Acknowledgments

The studies presented in this paper were carried out when the author was with the Communications Research Laboratory, Ministry of Posts and Telecommunications.

References

ASO, T., TSUDA, T., TAKASHIMA, Y., ITO, R. and KATO, S. (1980): Observations of lower ionospheric wind by the Kyoto meteor radar. J. Geophys. Res., **85**, 177-184.

BRISTOW, W.A., GREENWALD, R.A. and SAMSON, J.C. (1994): Identification of high-latitude acoustic gravity wave sources using the Goose Bay HF radar. J. Geophys. Res., **99**, 319-331.

CARTER, D.A. and BALSLEY, B.B. (1982): The summer wind field between 80 and 93 km observed by the MST radar at Poker Flat, Alaska (65°N). J. Atmos. Sci., **39**, 2905-2915.

DAVIES, K. and JONES, J.E. (1971): Three-dimensional observations of traveling ionospheric disturbances. J. Atmos. Terr. Phys., **33**, 39-46.

ELFORD, W.G. and MURRAY, E.L. (1960): Upper atmosphere wind measurements in the Antarctic. Space Research **I**, Amsterdam, North-Holland, 158-163.

EVANS, J.V., HOLT, J.M. and WAND, R.H. (1983): A differential-Doppler study of traveling ionospheric disturbances from Millstone Hill. Radio Sci., **18**, 435-451.

GLASS, M., BERNARD, R., FELLOUS, J.L. and MASSEBEUF, M. (1978): The French meteor radar facility. J. Atmos. Terr. Phys., **40**, 923-931.

GEORGES, T.M. and HOOKE, W.H. (1970): Wave-induced fluctuations in ionospheric electron content: A model indicating some observational biases. J. Geophys. Res., **75**, 6295-6308.

HIROTA, I. (1984): Climatology of gravity waves in the middle atmosphere. J. Atmos. Terr. Phys., **46**, 767-773.

HOCKE, K. and SCHLEGEL, K. (1996): A Review of atmospheric gravity waves and travelling ionospheric disturbances: 1982-1995. Ann. Geophys., **14**, 917-940.

HOOKE, W.H. (1970): The ionospheric response to internal gravity waves. 1. The F_2 region response. J. Geophys. Res., **75**, 5535-5544.

HUNSUCKER, R.D. (1982): Atmospheric gravity waves generated in the high-latitude ionosphere: A review. Rev. Geophys. Space Phys., **20**, 293-315.

IGARASHI, K., OGAWA, T., OSE, M., FUJII, R. and HIRASAWA, T. (1982): A new VHF Doppler radar experiment at Syowa Station, Antarctica. Mem. Natl Inst. Polar Res., Spec. Issue, **22**, 258-267.

NOMURA, A., KANO, T., IWASAKA, Y., FUKUNISHI, H., HIRASAWA, T. and KAWAGUCHI, S. (1987): Lidar observations of the mesospheric sodium layer at Syowa Station, Antarctica. Geophys. Res. Lett., **14**, 700-703.

NOMURA, A., IWASAKA, Y., FUKUNISHI, H., HIRASAWA, T. KAWAGUCHI, S. and KANO, T. (1988): Dynamics of the mesospheric sodium layer in Antarctica: Lidar measurements at Syowa Station, 1985. Proc. NIPR Symp. Upper Atmos. Phys., **1**, 75-83.

NOMURA, A., IWASAKA, Y. and KANO, T. (1989): Gravity wave activities over Syowa Station, Antarctica. Proc. NIPR Symp. Polar Meteorol. Glaciol., **2**, 1-7.

OGAWA, T. (1995): Syowa Station MF radar experiment for studying the Antarctic upper middle atmosphere: A proposal. Proc. NIPR Symp. Upper Atmos. Phys., **8**, 70-72.

OGAWA, T. (1996): Radar observations of ionospheric irregularities at Syowa Station, Antarctica: A brief overview. Ann. Geophys., **14**, 1454–1461.

OGAWA, T., IGARASHI, K., OSE, M., KURATANI, Y., FUJII, R. and HIRASAWA, T. (1983): Preliminary results of new 50 MHz Doppler radar experiment at Syowa Station. Mem. Natl Inst. Polar Res., Spec. Issue, **26**, 193–201.

OGAWA, T., IGARASHI, K., KURATANI, Y., FUJII, R. and HIRASAWA, T. (1985): Some initial results of 50 MHz meteor radar observation at Syowa Station. Mem. Natl Inst. Polar Res., Special Issue, **36**, 254–263.

OGAWA, T., IGARASHI, K., AIKYO, K. and MAENO, H. (1987): NNSS satellite observations of medium-scale traveling ionospheric disturbances at southern high-latitudes. J. Geomagn. Geoelectr., **39**, 709–721.

OGAWA, T., IGARASHI, K., AIKYO, K. and MAENO, H. (1988): Satellite observation of medium-scale traveling ionospheric disturbances over Syowa Station. Proc. NIPR Symp. Upper Atmos. Phys., **1**, 192–198.

OGAWA, T., NOMURA, A., TANAKA, T. and IGARASHI, K. (1989): Simultaneous measurements of Antarctic mesospheric gravity waves by meteor radar and lidar. J. Geomagn. Geoelectr., **41**, 835–849.

PRIKRYL, P., KOEHLER, J.A. and SOFKO, G.J. (1986): Simultaneous CW radio measurements of meteor and auroral drifts. Radio Sci., **21**, 271–282.

REID, G.C. (1983): The influence of electric fields on radar measurements of winds in the upper mesosphere. Radio Sci., **18**, 1028–1034.

RÖTTGER, J. and TSUDA, T. (1995): Studies of the polar middle and lower atmosphere by an MST radar on Svalbard. J. Geomagn. Geoelectr., **47**, 929–942.

TANAKA, T., OGAWA, T. and NOMURA, A. (1988): Neutral wind observation by 50MHz meteor radar at Syowa Station. Proc. NIPR Symp. Upper Atmos. Phys., **1**, 84–87.

TSUDA, T., MURAYAMA, T., NAKAMURA, T., VINCENT, R.A., MANSON, A.H., MEEK, C.E. and WILSON, R.L. (1994): Variations of the gravity wave characteristics with height, season and latitude revealed by comparative observations. J. Atmos. Terr. Phys., **56**, 555–568.

(Received April 18, 1997; Revised manuscript accepted June 25, 1997)